

Extracellular Calcium Regulates Postsynaptic Efficacy through Group 1 Metabotropic Glutamate Receptors

Neil R. Hardingham,¹ Neil J. Bannister,¹ Jenny C. A. Read,¹ Kevin D. Fox,² Giles E. Hardingham,³ and J. Julian B. Jack¹

¹The University Laboratory of Physiology, Oxford University, Oxford OX1 3PT, United Kingdom, ²The School of Biosciences, Cardiff University, Cardiff CF10 3US, United Kingdom, and ³Centre for Neuroscience Research, Royal (Dick) School of Veterinary Studies, University of Edinburgh, Edinburgh EH9 1QH, United Kingdom

Bursts of synaptic transmission are known to induce transient depletion of Ca^{2+} within the synaptic cleft. Although Ca^{2+} depletion has been shown to lower presynaptic release probability, effects on the postsynaptic cell have not been reported. In this study, we show that physiologically relevant reductions in extracellular Ca^{2+} lead to a decrease in synaptic strength between synaptically coupled layer 2/3 cortical pyramidal neurons. Using quantal analysis and mEPSP analysis, we demonstrate that a lowered extracellular Ca^{2+} produces a reduction in the postsynaptic quantal size in addition to its known effect on release probability. An elevated Mg^{2+} level can prevent this reduction in postsynaptic efficacy at subphysiological Ca^{2+} levels. We show that the calcium-dependent effect on postsynaptic quantal size is mediated by group 1 metabotropic glutamate receptors, acting via CaMKII (Ca^{2+} /calmodulin-dependent protein kinase II) and PKC. Therefore, physiologically relevant changes in extracellular Ca^{2+} can regulate information transfer at cortical synapses via both presynaptic and postsynaptic mechanisms.

Key words: calcium [Ca]; metabotropic glutamate receptor; cortex; postsynaptic; CaMK-II; protein kinase C α

Introduction

The role of Ca^{2+} ions is central to synaptic function, controlling both presynaptic release of neurotransmitter and induction of synaptic plasticity in the postsynaptic cell. There is mounting evidence that levels of extracellular calcium ($[\text{Ca}^{2+}]_{\text{ec}}$) in the synaptic cleft can fall after periods of neuronal activity. For example, application of excitatory amino acids to the neocortex can cause 15-fold reductions in $[\text{Ca}^{2+}]_{\text{ec}}$ to <0.1 mM (Pumain and Heinemann, 1985). Studies in the hippocampus have shown that, after a more physiological 10 Hz synaptic stimulation for several seconds, free $[\text{Ca}^{2+}]_{\text{ec}}$ can fall from 2 to 1.5 mM (Nicholson et al., 1977). A reduction in the size of the presynaptic Ca^{2+} current has been reported after a prolonged (100 ms pulse) depolarization of the presynaptic or postsynaptic membrane, which was attributed to Ca^{2+} depletion in the cleft (Borst and Sakmann, 1999). Modeling studies indicate that the degree of Ca^{2+} depletion is highly dependent on firing frequency (Vassilev et al., 1997). However, other factors such as receptor channel density, glia, and synapse size are also important. (Egelman and Montague, 1999; Rusakov, 2001). Detailed compartmental models of the synaptic cleft suggest that shifts in $[\text{Ca}^{2+}]_{\text{ec}}$ can occur after a single presynaptic action potential (Rusakov et al., 1999). The flow of Ca^{2+} through NMDA receptors also contributes to a reduction of available

Ca^{2+} ions in the synaptic cleft. (Egelman and Montague, 1998, 1999; Rusakov and Fine, 2003). Furthermore, dendritic spiking may also significantly deplete local Ca^{2+} (Wiest et al., 2000). It therefore appears that after synaptic stimulation both presynaptic and postsynaptic elements are competing for the available Ca^{2+} in the synaptic cleft.

Given this evidence of activity-dependent Ca^{2+} depletion at central synapses, we decided to examine how changes in $[\text{Ca}^{2+}]_{\text{ec}}$ may affect the strength of synapses between cortical pyramidal neurons in layer 2/3 of the rat visual cortex. To examine presynaptic and postsynaptic determinants, the trial-to-trial distribution of EPSP amplitudes were subjected to a quantal analysis (Del Castillo and Katz, 1954). Quantal analysis has been used with reluctance at central synapses because of problems of nonuniform release probability (Walmsley et al., 1988) and high quantal variance (Stricker and Redman, 2003). However, using brain slices from more mature animals greatly reduces quantal variance (Wall and Usowicz, 1998). Studies in the hippocampus have suggested that quantal variance is low enough to attempt an analysis between 3 and 4 weeks of age (Stricker et al., 1996). In addition, it has also been shown recently that release probabilities at different boutons of a given layer 2/3 pyramidal connection in the rat neocortex are comparable (Koester and Johnston, 2005), suggesting that a simple binomial model of transmitter release may be a valid description at these synapses.

A quantal analysis of layer 2/3 excitatory cortical connections reveals that, in addition to the reduction in presynaptic efficacy, a drop in $[\text{Ca}^{2+}]_{\text{ec}}$ causes a significant reduction in quantal size (a measure of postsynaptic efficacy), which is

Received Dec. 2, 2005; revised May 4, 2006; accepted May 4, 2006.

This work was supported by The Wellcome Trust, The Medical Research Council (United Kingdom), and the Royal Society.

Correspondence should be addressed to Dr. Neil R. Hardingham, Biosci 3, The School of Biosciences, Cardiff University, Museum Avenue, Cardiff CF10 3US, UK. E-mail: sbinrh@cardiff.ac.uk.

DOI:10.1523/JNEUROSCI.5128-05.2006

Copyright © 2006 Society for Neuroscience 0270-6474/06/266337-09\$15.00/0

mediated via postsynaptic group 1 metabotropic glutamate receptors (mGluR1s).

Materials and Methods

Slice preparation and intracellular recording. All recordings were made from brain slices taken from 19- to 27-d-old Sprague Dawley rats. Animals were killed by cervical dislocation and parasagittal slices of visual cortex (400 μm thick) were prepared by conventional methods (Hardingham and Larkman, 1998). Slices were maintained at 23°C in artificial CSF (ACSF) containing the following (in mM): 119 NaCl, 3.5 KCl, 1 NaH_2PO_4 , 2.5 CaCl_2 , 1 MgSO_4 , 26 NaHCO_3 , and 10 glucose, bubbled with 95% O_2 and 5% CO_2 .

Whole-cell voltage recordings were made from the somata of closely adjacent pairs of pyramidal neurons within layer 2/3 (predominantly layer 2) of the visual cortex, selected by near-infrared differential interference contrast video microscopy (Dodt and Zieglansberger, 1990) using a Zeiss (Oberkochen, Germany) Axioskop upright microscope equipped with a 40 \times water-immersion objective. Recording pipettes contained the following (in mM): 110 potassium gluconate, 10 KCl, 2 MgCl_2 , 2 Na_2ATP , 10 EGTA, 2 CaCl_2 and 10 HEPES, adjusted to pH 7.3, and 270 mOsm. Before seal formation, neurons were selected as pyramidal by the presence of a prominent apical dendrite. Subsequently, the neuron could be identified as a pyramid by its asymmetric spikes, typical of pyramidal neurons in this layer (McCormick et al., 1985; Mason et al., 1991).

Single action potentials were elicited (by current injection) in one neuron and on-line spike-triggered averaging was used to detect any resultant EPSP elicited in the other neuron. If no EPSP could be detected, the pair of cells was tested for a connection in the other direction. Once a synaptic connection had been identified, single action potentials were induced in the presynaptic cell at 0.1 or 0.2 Hz by injection of short (5–10 ms) pulses of depolarizing current. Postsynaptic responses were amplified, low-pass filtered at 2 kHz, digitized at 5 kHz using a CED (Cambridge Electronic Design, Cambridge, UK) 1401 analog-to-digital board and recorded on a PC for analysis off-line. Postsynaptic neurons were held at membrane potentials more negative than -70 mV to ensure that EPSPs were dominated by AMPA currents but holding current was rarely necessary. Slices were continually perfused with ACSF during recording.

After control periods of recording at 2.5 mM $[\text{Ca}^{2+}]_{\text{ec}}$, the $[\text{Ca}^{2+}]_{\text{ec}}$ and in some cases $[\text{Mg}^{2+}]_{\text{ec}}$ were changed by perfusing the recording bath with an ACSF solution containing a different concentration of cation(s) and/or other drugs. At least 20 min of recordings were made after each solution change to ensure equilibration. To verify that changes in divalent cation concentrations were not mediating their effects via changes in the membrane properties of cells, we monitored the input resistance (R_{in}) and membrane time constant of the cell (τ_{m}). No significant change in either R_{in} or τ_{m} was observed after the changes we made to the ionic composition of the ACSF.

AP5 (50 μM), picrotoxin (100 μM), TTX (1 μM), AP3 (1 mM), 7-(hydroxyimino)cyclopropachromen-1 α -carboxylateethyl ester (CPC-COEt; 50 μM) and (RS)-3,5-dihydroxyphenylglycine (DHPG; 100 μM) were bath applied. Pertussis toxin (1 $\mu\text{g}/\text{ml}$), 2-[1-(3-dimethylamino-propyl)-1H-indol-3-yl]-3-(1H-indol-3-yl)maleimide (GF109203X; 100 μM), 1-[N,Q-bis(5-isoquinolinesulfonyl)-N-methyl-L-tyrosyl]-4-phenylpiperazine (KN62) (50 μM), N-(2-aminoethyl)-5-isoquinolinesulfonamide hydrochloride (H9) (10 μM), microcystin (10 μM), and cyclosporin (10 μM) were all applied intracellularly via the patch electrode. All drugs were purchased from Tocris (Bristol, UK).

Measurement of EPSP amplitude. For each EPSP recorded, the peak amplitude from each spike-triggered sweep was measured off-line using a computer routine that compared the average voltage during a 0.4–2 ms period of baseline potential with the average voltage during a period of the same duration at the EPSP peak. For each EPSP, the measurement windows were determined from the averaged EPSP waveform. Measurements of noise were obtained using the same time windows used to measure the EPSP, but implemented in an area of baseline remote from the EPSP. At least three separate noise measurements were taken for each EPSP from nonoverlapping parts of the baseline to calculate the mean noise SD. This noise SD was subtracted from the EPSP SD using the

equation $(\text{EPSP SD})^2 = (\text{SD of combined EPSP} + \text{noise})^2 - (\text{noise SD})^2$. To verify that the postsynaptic changes in EPSP amplitude we observed in these experiments were changes in AMPA currents, we sought to verify that the EPSPs we were recording at -70 mV were exclusively AMPA mediated. In 50 μM APV, EPSPs were on average 1.06 ± 0.04 times their control value ($n = 5$). Therefore NMDA receptors do not appear to contribute significantly to EPSPs recorded at -70 mV.

Selection of EPSP data. Only EPSP recordings remaining stable for at least 100 consecutive trials of the control period of recording were included in the final data set. Stable periods of data were defined as those in which the mean and SD, taken over successive epochs of 50 trials, remained close to their values for the first epoch. The SD was required to remain within 30% of its initial value, whereas the mean amplitude was required to remain within three times the SE of the first epoch (approximately ± 0.5 SD). A study in the hippocampus has suggested that there could be significant drifts in quantal size over time (Larkman et al., 1997), which were sometimes associated with inverse changes in release probability, with no net effect on the mean amplitude (A.U. Larkman, unpublished observations). This possibility is minimized by imposing stability criteria on the SD as well as on the mean amplitude because, for a binomial process, changes in release probability only minimally affect the SD, whereas changes in quantal size have a much greater effect on the SD.

Extracting quantal parameters. Histograms of amplitude frequency distributions of EPSPs from stable periods of data often ($\approx 50\%$ of recordings) contained regularly spaced peaks, indicative of a quantal release of neurotransmitter at the synapses. It has been shown that neocortical synapses relating to individual connections appear to operate with similar release probabilities, which are target derived (Koester and Johnston, 2005) and so can be approximated with a simple binomial model. Therefore, the working hypothesis was that the EPSP amplitudes were drawn from a simple binomial distribution characterized by the number of release sites (N), release probability (P_r), and quantal size (Q) (Larkman et al., 1997). Experimental noise was represented as a Gaussian with SD σ_n . We incorporated an offset S to allow for the fact that the mean amplitude of failures may differ slightly from zero, because of extracellular field effects (Stricker et al., 1996). Finally, we included a parameter σ_Q representing quantal variance.

Models were fitted to experimental data using the method of maximum likelihood (Press et al., 1993). The noise σ_n was obtained by fitting a single Gaussian function to a noise distribution measured from the postsynaptic neuron. For a given number of release sites, N , the continuously variable parameters (P_r , Q , σ_Q , S) were then fitted to the data so as to maximize the likelihood (L_N). The optimal N was defined to be that with the highest L_N . Starting from $N = 1$, N was increased until it was either four larger than the N value with the highest L_N so far encountered, or 20, whichever occurred first.

Locating a global maximum in a multidimensional parameter space is a nontrivial matter. It was performed with the `fminsearch` algorithm from MATLAB's Optimization Toolbox. To guard against being misled by a local maximum, every fit was repeated with 10 different randomly chosen starting positions in the parameter space. During development, the performance of this algorithm was validated against a simulated annealing algorithm (Press et al., 1993) implemented in C++, repeated with three different cooling regimes (J. C. Read, unpublished observation).

For each EPSP recording in the final data set, we fitted at least one period of stable data (recorded in 2.5 mM $[\text{Ca}^{2+}]_{\text{ec}}$) with a simple binomial model. This provided us with a model for the connection at 2.5 mM $[\text{Ca}^{2+}]_{\text{ec}}$ including the number of release sites (N), the release probability (P_r), and the quantal size (Q). We made the assumption that N remained constant during the remainder of the recording, and so could be constrained in subsequent fits to the remaining data sets from that connection.

Adequacy of fitted model. To test whether the proposed fit was acceptable as a model of the experimental data, seven goodness-of-fit statistics were considered: the Kolmogorov–Smirnov D statistic (Press et al., 1993), the sum of the squared differences between the model and data cumulative distributions, and the χ^2 statistic for five different bin sizes. The power of the χ^2 statistic depends strongly on the bin size used. With

too few bins, the test is too coarse to catch local deviations of the data from the model predictions. Conversely, if too many bins are used, the number of data points falling in any one bin is small and subject to large sampling fluctuations, so the statistic again tolerates poor fits. The optimal number of bins depends on the data set. By using a range of different bin numbers (20, 30, 50, 75, and 100) for each data set, we ensured that each data set would be exposed to a rigorous test. The distributions of these statistics under the null hypothesis, that the experimental data had actually been drawn from the fitted model, were obtained by Monte Carlo simulation (implemented in MATLAB on a personal computer). Five thousand sets of simulated data, each the same size as the experimental data set, were generated from the fitted model, and the seven goodness-of-fit statistics were calculated for each simulated data set. For each statistic, we calculated what proportion (f) of simulated data sets yielded higher values of the statistic (indicating worse fits) than the experimental data. A value of $f > 5\%$ means that the null hypothesis cannot be rejected at the 5% level on the basis of the statistic. Finally, we applied an additional test, using the proportion of events that failed to evoke a simulated EPSP, p_{fail} . The Monte Carlo distribution of failure rates could then be compared with the p_{fail} observed experimentally. The failure rate test is a two-tailed test, so the null hypothesis is accepted at the 5% level provided that the experimental p_{fail} lies in between the 2.5 and 97.5% quantiles of the Monte Carlo distribution. The quantal models describing each period of experimental data were not accepted if any of our tests provided evidence to reject the null hypothesis at the 5% level. For approximately half of our recordings, we were unable to obtain a satisfactory binomial model, similar to the proportion reported by (Koester and Johnston, 2005). This was either as a result of the fitting algorithm being unable to compute an optimal solution, or because the model failed on one or more of the rigorous statistical tests.

Miniature EPSPs. Miniature EPSPs (mEPSPs) were recorded from a different population of layer 2/3 pyramidal neurons at 2.5 mM $[\text{Ca}^{2+}]_{\text{ec}}/1$ mM $[\text{Mg}^{2+}]_{\text{ec}}$ and 1 mM $[\text{Ca}^{2+}]_{\text{ec}}/1$ mM $[\text{Mg}^{2+}]_{\text{ec}}$ in the presence of 50 μM APV, 1 μM TTX, and 100 μM picrotoxin. The mEPSP files were analyzed blind and EPSPs were identified by eye on the basis of their rapid rise and slow decay times. Their amplitudes were determined using a computer optimizing routine that fitted the sum of two exponential functions (rise and decay) to each mEPSP (Hardingham and Larkman, 1998). A total of 250 mEPSPs were measured for each of four neurons and pooled to give an mEPSP amplitude distribution of 1000 events, initially at 2.5 mM $\text{Ca}^{2+}_{\text{ec}}$, then at 1.0 mM $\text{Ca}^{2+}_{\text{ec}}$, and then again at 2.5 mM. This experiment was performed at both 23 and 34°C.

Unless otherwise stated, values quoted are mean \pm SEM. Statistical tests for differences between populations were made using paired t tests.

Results

EPSP size behaves as a function of $[\text{Ca}^{2+}]_{\text{ec}}$

To investigate the effect of $[\text{Ca}^{2+}]_{\text{ec}}$ on synaptic efficacy, we recorded EPSPs from synaptically connected layer 2/3 cells in supraphysiological (2.5 mM) and subphysiological (1 mM) $[\text{Ca}^{2+}]_{\text{ec}}$, maintaining $[\text{Mg}^{2+}]_{\text{ec}}$ at 1 mM (Fig. 1). In all cases, the mean EPSP amplitude dropped after $[\text{Ca}^{2+}]_{\text{ec}}$ was lowered. On average, the mean EPSP amplitude recorded in 1.0 mM $[\text{Ca}^{2+}]_{\text{ec}}$ was a quarter ($26 \pm 3\%$) of that recorded in 2.5 mM $[\text{Ca}^{2+}]_{\text{ec}}$ (Fig. 1c) ($n = 10$). On returning to 2.5 mM $[\text{Ca}^{2+}]_{\text{ec}}$, the mean EPSP amplitude returned to close to the initial value observed before the drop in $[\text{Ca}^{2+}]_{\text{ec}}$ (Fig. 1).

To investigate in detail the locus of the change in synaptic efficacy, we used quantal analysis methods. Optimal binomial model fits to EPSP amplitude histograms recorded in 2.5 mM $[\text{Ca}^{2+}]_{\text{ec}}$ returned values for quantal size (Q) that were consistent with the spacings between peaks from Gaussian filtered histograms (Figs. 2a,b). We were unable to obtain a simple binomial model fit to approximately half of our recorded synaptic connections, consistent with previous studies (Koester and Johnston, 2005). The mean quantal amplitude (Q) obtained from these fits at 2.5 mM $[\text{Ca}^{2+}]_{\text{ec}}$ was $271 \pm 21 \mu\text{V}$ ($n = 10$ connections). To

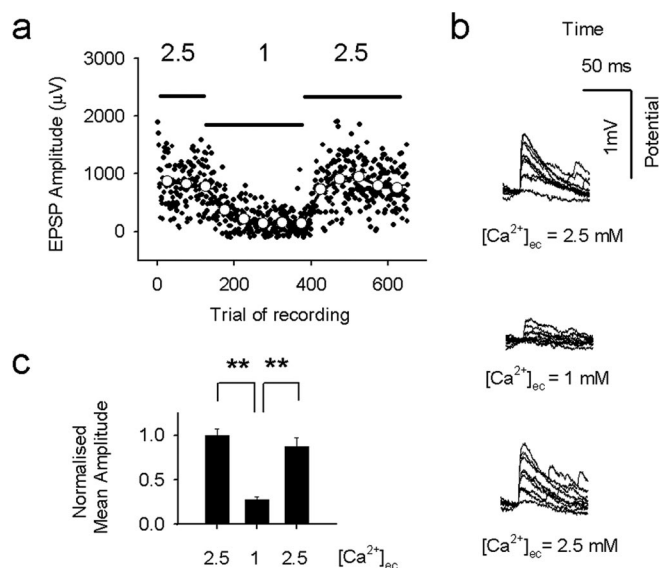


Figure 1. Extracellular $[\text{Ca}^{2+}]_{\text{ec}}$ regulates EPSP amplitude of paired recordings between layer 2/3 neurons. **a**, Trial-to-trial measurements of EPSP amplitudes (filled circles) and mean EPSP amplitude per 50 trial epoch (open circles) from a single experiment. Recordings were first made in ACSF containing 2.5 mM $[\text{Ca}^{2+}]_{\text{ec}}$ (150 trials), and then 1 mM $[\text{Ca}^{2+}]_{\text{ec}}$ (250 trials) and back to 2.5 mM $[\text{Ca}^{2+}]_{\text{ec}}$ (250 trials). $[\text{Mg}^{2+}]_{\text{ec}}$ was maintained at 1 mM throughout. **b**, Individual traces taken from periods of stable recording in each $[\text{Ca}^{2+}]_{\text{ec}}$. For each example, 10 consecutive EPSPs are overlaid. **c**, Summary data showing the effect of $[\text{Ca}^{2+}]_{\text{ec}}$ on mean EPSP amplitude (normalized, $n = 10$). $**p < 0.01$. Error bars indicate SE.

verify that the derived models yielded realistic values for Q , we compared estimates for Q (derived from modeling) with amplitudes of spontaneous miniature EPSPs (mEPSPs) recorded from similar cells in TTX, APV, and picrotoxin. The mean amplitude of mEPSPs (from four cells) was $298 \pm 4 \mu\text{V}$ ($n = 500$), which was not significantly different to the derived values of quantal size ($p > 0.05$), suggesting that the values obtained for Q were reliable measurements of single vesicular release.

Our initial assumption was that the reduction in mean EPSP amplitude observed when $[\text{Ca}^{2+}]_{\text{ec}}$ was lowered from 2.5 to 1 mM was purely attributable to a reduction in release probability (a presynaptic effect). The presynaptic Ca^{2+} current (I_{Ca}) has been previously shown to be proportional to $[\text{Ca}^{2+}]_{\text{ec}}$ (i.e., $I_{\text{Ca}} \propto [\text{Ca}^{2+}]_{\text{ec}}$) (Mintz et al., 1995). An entirely presynaptic change would involve no postsynaptic change (in Q) on varying $[\text{Ca}^{2+}]_{\text{ec}}$. To test this hypothesis, stable periods of data recorded during periods of low $[\text{Ca}^{2+}]_{\text{ec}}$ (1 mM) were fitted with a binomial model constraining Q to the value derived from the same connection in 2.5 mM Ca^{2+} . In all cases ($n = 10$), models constraining Q to $Q_{2.5}$ were inadequate in describing the 1 mM Ca^{2+} data (Fig. 2c). When the data were refitted, this time allowing Q to optimize, adequate fits were returned with smaller Q values than obtained at 2.5 mM Ca^{2+} (Fig. 2d). On average, the mean quantal size at 1.0 mM $[\text{Ca}^{2+}]_{\text{ec}}$ was $64 \pm 4\%$ of that measured from the same connection recorded in 2.5 mM $[\text{Ca}^{2+}]_{\text{ec}}$ (Fig. 2e).

To confirm that the reduction in Q with $[\text{Ca}^{2+}]_{\text{ec}}$ was reversible, for each connection, we recorded a second period of data in 2.5 mM $[\text{Ca}^{2+}]_{\text{ec}}$. In all cases, models fitted to this later period of data in 2.5 mM Ca^{2+} constraining Q to that recorded in 1 mM Ca^{2+} were again found to be inadequate ($n = 10$) (supplemental Fig. 1e, available at www.jneurosci.org as supplemental material). However, models constraining Q to that recorded initially in 2.5 mM $[\text{Ca}^{2+}]_{\text{ec}}$ were considered adequate (supplemental Fig. 1, available at www.jneurosci.org as supplemental material). Con-

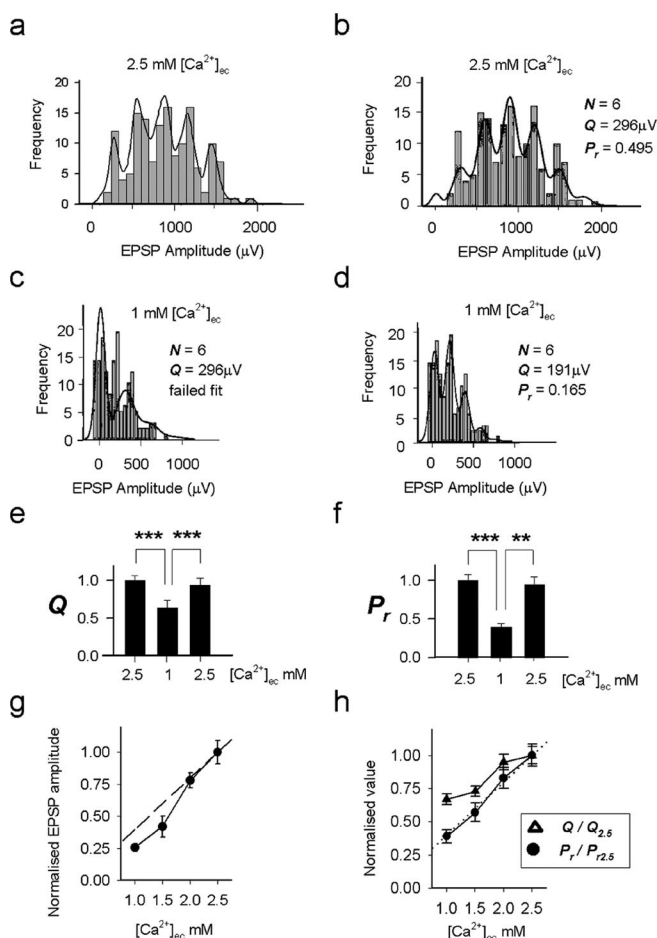


Figure 2. $[Ca^{2+}]_{ec}$ regulates quantal size as well as release probability. **a**, Amplitude frequency histogram for the first stable period of data shown in Figure 1 (vertical bars, recorded in 2.5 mM Ca^{2+}) and a Gaussian filtered version of it (solid line). **b**, The highest likelihood quantal model (solid line) shows similar peak spacing to the filtered data and is adequate in describing the data. Values for the number of release sites (N), quantal size (Q) and release probability (P_r) predicted by the model are given. **c**, The highest likelihood quantal model constraining Q to $Q_{2.5}$ ($296 \mu V$) is inadequate in describing data recorded from the same connection at 1 mM $[Ca^{2+}]_{ec}$. **d**, The highest likelihood quantal model allowing free fitting of Q successfully fits the 1 mM $[Ca^{2+}]_{ec}$ data with a much lower Q of $191 \mu V$. **e**, Summary data showing the effect of $[Ca^{2+}]_{ec}$ on quantal size ($n = 10$ connections, values normalized to initial recording in 2.5 mM Ca^{2+}). **f**, Summary data showing the effect of $[Ca^{2+}]_{ec}$ on release probability ($n = 10$ connections, values normalized to initial recording in 2.5 mM Ca^{2+}). **g**, Relationship between mean EPSP amplitude and $[Ca^{2+}]_{ec}$. Amplitudes are normalized to data recorded in 2.5 mM $[Ca^{2+}]_{ec}$. **h**, Relationship between $Q/[Ca^{2+}]_{ec}$ and $P_r/[Ca^{2+}]_{ec}$. Values are normalized to data recorded in $[Ca^{2+}]_{ec}$. Error bars indicate SE. ** $p < 0.01$; *** $p < 0.001$

sistent with this result, subsequent fits to the second epoch of data recorded in 2.5 mM $[Ca^{2+}]_{ec}$, this time allowing Q to optimize, returned values for Q that were similar to the initial values of Q recorded in 2.5 mM $[Ca^{2+}]_{ec}$ ($93.9 \pm 5.1\%$) (Fig. 2e, supplemental Fig. 1, available at www.jneurosci.org as supplemental material). These results provide evidence of considerable (and reversible) postsynaptic modification in response to lowering $[Ca^{2+}]_{ec}$ from 2.5 to 1 mM.

In addition to obtaining values for quantal size (Q) from EPSP recordings, we also derived values for P_r . The mean release probability in 2.5 mM $[Ca^{2+}]_{ec}$ was 0.50 ± 0.05 ($n = 10$). Mean P_r dropped to 0.17 ± 0.01 in 1 mM $[Ca^{2+}]_{ec}$ (a reduction of $61 \pm 4\%$; $n = 10$) (Fig. 2f). This reduction is very similar to the drop in P_r that would be seen if there was a linear relationship between $[Ca^{2+}]_{ec}$ and synaptic release. The failure rate for EPSPs at 2.5

mM $[Ca^{2+}]_{ec}$ was 0.17 ± 0.04 , which is consistent with that reported for paired recordings from layer V pyramidal connections in rat cortex of similar age (Markram et al., 1997). The mean number of release sites (N), derived from quantal analysis methods, was 3.9 ± 0.8 , which is again similar to the number of contacts that have been found between paired cortical neurons, assuming one functional synapse per anatomical connection (Feldmeyer et al., 1999).

We next sought to investigate in more detail the relationship between $[Ca^{2+}]_{ec}$ and synaptic parameters P_r and Q . EPSPs were recorded in a series of $[Ca^{2+}]_{ec}$ from 1 to 2.5 mM (Figs. 2g,h) ($n = 8$ connections). Data recorded at each $[Ca^{2+}]_{ec}$ were fitted with a binomial model allowing the estimate of Q to be optimized. The relationship of mean EPSP amplitude with $[Ca^{2+}]_{ec}$ showed a slope greater than unity, especially between 1.5 and 2 mM $[Ca^{2+}]_{ec}$ (Fig. 2g), but when changes in mean amplitudes were separated into changes in Q and P_r , neither slope was significantly greater than unity (Fig. 2h). This finding suggests an absence of cooperativity between $[Ca^{2+}]_{ec}$ and vesicular release at cortical synapses, because P_r appears only to increase linearly with $[Ca^{2+}]_{ec}$. Quantal amplitudes were as follows: $0.67 \pm 0.04 Q_{2.5}$ at 1 mM $[Ca^{2+}]_{ec}$, $0.73 \pm 0.04 Q_{2.5}$ at 1.5 mM $[Ca^{2+}]_{ec}$, and $0.95 \pm 0.05 Q_{2.5}$ at 2.0 mM $[Ca^{2+}]_{ec}$ (Fig. 2h).

mEPSP amplitudes show a similar dependence on extracellular calcium to Q

We next sought to confirm our findings regarding the change in Q with $[Ca^{2+}]_{ec}$ using an alternative technique. Miniature EPSPs (mEPSPs) are triggered by single spontaneous vesicular releases at excitatory synapses and provide an alternative means to measure quantal size.

The mean amplitude of mEPSP, recorded in TTX, APV, and picrotoxin, dropped by $32 \pm 2\%$ after a reduction in $[Ca^{2+}]_{ec}$ from 2.5 to 1 mM (Fig. 3a). This is comparable with the reduction in quantal amplitude observed in connections between synaptically coupled pairs of neurons ($36 \pm 4\%$). Experiments performed at more physiological temperatures ($34^\circ C$) again showed very similar changes (Fig. 3b) ($28 \pm 2\%$), and the effect was also reversible. mEPSPs had average 10–90% rise times of 3.5 ± 0.04 ms ($n = 2000$), which were again highly comparable with the rise times of EPSPs from paired recordings [mean 10–90% rise time, 3.3 ± 0.2 ms ($n = 10$)]. We were therefore satisfied that the two experimental approaches were sampling from the same population of synapses. mEPSPs are widely regarded to be unquantal, and changes in amplitude reflect a postsynaptic modification. However, an alternative explanation of our data is that a proportion of mEPSPs recorded at 2.5 mM Ca^{2+} are multiquantal, and the apparent change in quantal size with calcium represents a presynaptic effect. To investigate this possibility, we plotted amplitude frequency distribution plots for mEPSPs at 2.5 and 1 mM Ca^{2+} and measured their median and skew values (Fig. 3c,d). At 1 mM Ca^{2+} , median values showed a comparable drop to mean amplitude from that obtained at 2.5 mM Ca^{2+} [$68 \pm 4\%$, $23^\circ C$ (Fig. 3d) and $71 \pm 3\%$, $34^\circ C$ (data not shown)] whereas skew values were unchanged [$106 \pm 9\%$, $23^\circ C$ (Fig. 3d) and $105 \pm 14\%$, $34^\circ C$ (data not shown)]. This is consistent with a postsynaptic effect because any presynaptic effect would result in a change in the skew of the distribution and a greater change in median than mean amplitude.

$[Mg^{2+}]_{ec}$ can replicate the postsynaptic effect of $[Ca^{2+}]_{ec}$
Previous studies investigating the role of extracellular Ca^{2+} on synaptic function compensated for the reduction in divalent cat-

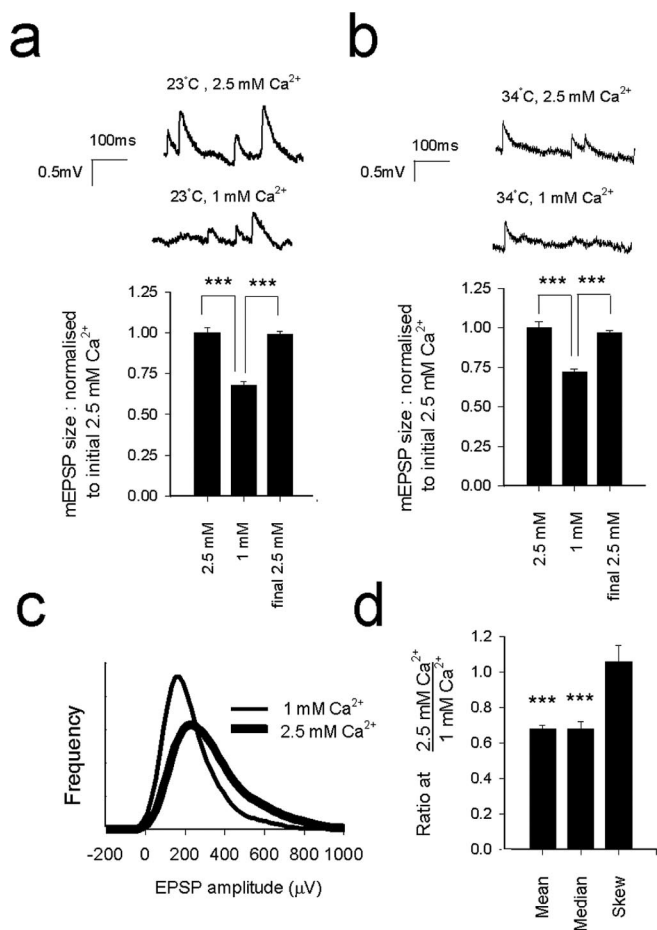


Figure 3. The effect of $[Ca^{2+}]_{ec}$ on mEPSPs. The effect of reducing $[Ca^{2+}]_{ec}$ from 2.5 to 1 mM on miniature EPSPs recorded in TTX, picrotoxin, and APV is shown in **a** at 23°C and in **b** at 34°C. Example traces are shown at both temperatures. **c**, The effect of $[Ca^{2+}]_{ec}$ on the mEPSP amplitude distribution from a single cell is illustrated. Individual amplitudes are filtered with a Gaussian (data recorded at 23°C). **d**, Effect of lowered $[Ca^{2+}]_{ec}$ on median amplitude of the distributions is comparable with the effect of $[Ca^{2+}]_{ec}$ on the mean amplitude, although there is no effect on the skew of the distributions (data recorded at 23°C). Effects on median amplitude and skew were comparable at 34°C (data not shown). Statistics given are comparisons between mEPSP populations recorded at 2.5 and 1.0 mM Ca^{2+} . Error bars indicate SE. **** $p < 0.001$.

ions by an elevated $[Mg^{2+}]_{ec}$ (Silver et al., 2003). This substitution does not presumably occur *in vivo* where, if anything, $[Mg^{2+}]_{ec}$ would also fall slightly after synaptic stimulation. We therefore investigated whether the postsynaptic effects brought about by lowering $[Ca^{2+}]_{ec}$ could be prevented by compensatory increases in $[Mg^{2+}]_{ec}$. Conventionally, Ca^{2+} is replaced with twice the amount of Mg^{2+} because of the weaker Mg^{2+} surface charge effects (Hille et al., 1975). To investigate this idea, EPSPs were recorded in a series of three different extracellular divalent ion concentration combinations (2.5 mM Ca^{2+} :1 mM Mg^{2+} ; 1 mM Ca^{2+} :1 mM Mg^{2+} ; and 1 mM Ca^{2+} :4 mM Mg^{2+} ; $n = 8$ cells) (Fig. 4). In all cases, models constraining Q to that measured in 2.5 Ca^{2+} :1 Mg^{2+} were adequate in describing the data in 1 Ca^{2+} :4 Mg^{2+} (Fig. 4a), but inadequate in describing the data in 1 Ca^{2+} :1 Mg^{2+} . Models fitted to data recorded in 1 Ca^{2+} :4 Mg^{2+} , allowing optimal fitting of Q , returned values for Q that were close to $Q_{2.5Ca}$ (0.93 ± 0.07) (Fig. 4b). Reductions in P_r from 2.5 Ca^{2+} :1 Mg^{2+} to 1 Ca^{2+} :4 Mg^{2+} were slightly larger than in 1 Ca^{2+} :4 Mg^{2+} , which might be expected from the antagonistic action of the Mg^{2+} ion on synaptic release (Fig. 4c). Therefore,

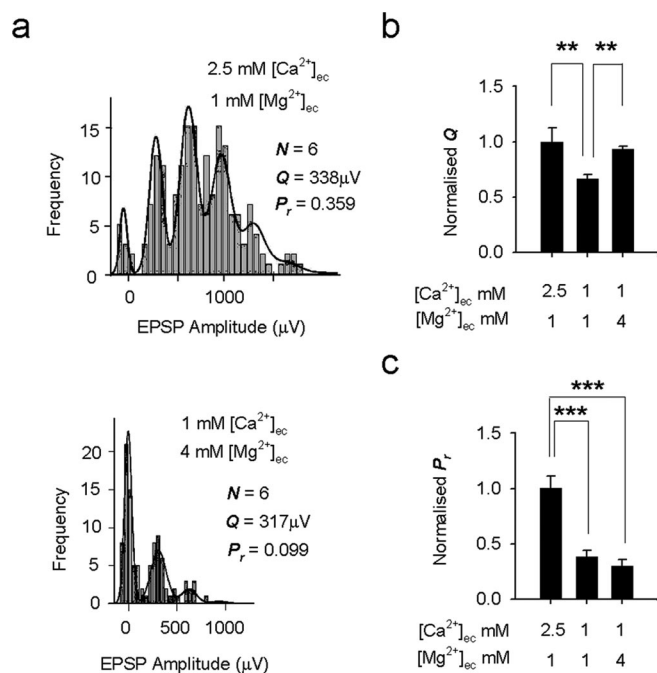


Figure 4. The reduction in Q on lowering $[Ca^{2+}]_{ec}$ is prevented by elevated $[Mg^{2+}]_{ec}$. **a**, EPSP amplitude frequency distributions (filtered) from recordings made in 2.5 mM $[Ca^{2+}]_{ec}$ /1 mM $[Mg^{2+}]_{ec}$ (top) and 1 mM $[Ca^{2+}]_{ec}$ /4 mM $[Mg^{2+}]_{ec}$ (bottom) taken from a single experiment. The model fit for each distribution is indicated by a solid line, with values for N , P_r , and Q shown. Summary data shows the effect of divalent ion concentration ($[Ca^{2+}]_{ec}$ and $[Mg^{2+}]_{ec}$) on quantal size (**b**) and release probability (**c**) ($n = 8$ connections), with values normalized to initial values obtained in 2.5 mM $[Ca^{2+}]_{ec}$ /1 mM $[Mg^{2+}]_{ec}$. Error bars indicate SE. ** $p < 0.01$; *** $p < 0.001$.

compensating surface charge by elevating $[Mg^{2+}]_{ec}$ largely blocks the reduction in Q seen in subphysiological $[Ca^{2+}]_{ec}$. This may explain why the postsynaptic effects of changes in $[Ca^{2+}]_{ec}$ have not been previously detected.

mGluR1 mediates the effect of $[Ca^{2+}]_{ec}$ on Q

We next investigated the signaling mechanism by which $[Ca^{2+}]_{ec}$ regulates Q . One possibility is the postsynaptic mGluR, which has been shown to be sensitive to both glutamate and Ca^{2+}_{ec} , and the IC_{50} for Ca^{2+} is within the physiological range of the synaptic cleft (Kubo et al., 1998; Francesconi and Duvoisin, 2004). Potentiating effects of mGluRs on excitatory cortical transmission have been demonstrated previously (Wang and Daw, 1996; Bandrowski et al., 2001; Jin et al., 2001; Iserhot et al., 2004); the most likely mGluRs to be involved in this process are the group 1 mGluRs, which are exclusively located postsynaptically (Lujan et al., 1997). Furthermore, mGluR1 has been shown to be activated by Mg^{2+} as well as Ca^{2+} (Francesconi and Duvoisin, 2004), making them worthy of investigation given our observation in Figure 4.

In recordings made in 2.5 mM $[Ca^{2+}]_{ec}$, bath application of either AP3 (a group 1 mGluR antagonist; $n = 7$) or CPCCOEt (a specific antagonist of mGluR1; $n = 3$) produced similar reductions in Q to those observed on reducing $[Ca^{2+}]_{ec}$ from 2.5 to 1 mM (compare Figs. 2e, 5a). Bath application of the selective group 1 mGluR agonist (DHPG; $n = 10$), however, had no significant effect on Q (Fig. 5a) when compared with control conditions. Conversely, at low (1 mM) $[Ca^{2+}]_{ec}$, application of AP3 ($n = 5$) produced no change in Q , whereas DHPG ($n = 5$) produced a significant Q increase (Fig. 5b). This increase in Q was similar to that observed on increasing $[Ca^{2+}]_{ec}$ from 1 to 2.5 mM (Fig. 2e).

Inclusion of DHPG in the bath solution prevented the drop in Q normally observed when $[Ca^{2+}]_{ec}$ was reduced from 2.5 to 1 mM ($n = 6$) (Fig. 5, compare *c*, top and bottom, *d*), but had no effect on the drop in P_r observed (Fig. 5*e*) ($n = 6$). Therefore, it appears that the control of Q by $[Ca^{2+}]_{ec}$ is mediated by mGluRs that have low activity at 1 mM $[Ca^{2+}]_{ec}$ and higher activity at 2.5 mM $[Ca^{2+}]_{ec}$. Application of either of the group 1 antagonists AP3 or CPCCOEt, or the group 1 agonist DHPG had no significant effect on P_r , either at 2.5 or 1 mM $[Ca^{2+}]_{ec}$ (data not shown).

Canonical group 1 mGluR signaling regulates Q via $[Ca^{2+}]_{ec}$

Activation of group 1 mGluRs is known to increase levels of active PKC and Ca^{2+} /calmodulin-dependent protein kinase II (CaMKII) via liberation of DAG and IP_3 respectively, through the activation of phospholipase C via Gq (Gudermann et al., 1996). PKC and CaMKII are known to be capable of modulation of AMPA channels (Carroll et al., 1998). In a final series of experiments, we sought to explore the signaling cascades that were mediating the $[Ca^{2+}]_{ec}$ /mGluR1 effect downstream of the mGluRs.

In these experiments, measures of Q were made from EPSPs initially recorded in 1 mM $[Ca^{2+}]_{ec}$ and then at 2.5 mM $[Ca^{2+}]_{ec}$. Under control conditions, Q increased by 39% when $[Ca^{2+}]_{ec}$ was thus increased (mean $Q_{2.5[Ca]}:Q_{1[Ca]}$ ratio was 1.39 ± 0.05) (Fig. 6*a*). The inclusion of pertussis toxin (a G-protein inhibitor) in the patch pipette ($n = 5$ cells), blocked this increase in Q (Fig. 6*a*). Equally, inclusion of the CaMKII inhibitor (KN62; $n = 4$ cells) or PKC inhibitor (GF109203X; $n = 4$) in the patch pipette blocked the increase in quantal size (Fig. 6*a*). In contrast, the PKA inhibitor (H9; $n = 4$ cells) had no significant effect on the Q/Ca^{2+} change (Fig. 6*a*).

As well as establishing the postsynaptic kinases involved in phosphorylating the AMPA channels and increasing Q on elevating $[Ca^{2+}]_{ec}$, we were also interested in establishing the counterbalancing phosphatases involved in the reduction of Q on lowering $[Ca^{2+}]_{ec}$.

Microcystin was used to inhibit protein phosphatases 1 and 2A (Thomas et al. 1997). This blocked the reduction in Q on lowering $[Ca^{2+}]_{ec}$ (Fig. 6*b*) ($n = 4$). Cyclosporin was used to block protein phosphatase 2B (Thomas et al., 1997). This drug had no effect on the reduction in Q observed in going from supra-physiological to subphysiological $[Ca^{2+}]_{ec}$ (Fig. 6*b*) ($n = 4$).

Discussion

Our key finding is that variations of $[Ca^{2+}]_{ec}$ within the physiological range can affect quantal size as well as the probability of release at central synapses. Effects of Ca^{2+} on synaptic release at both central and peripheral synapses are well documented (Augustine, 2001) but effects on Q have been largely overlooked up to now. Although the effect of $[Ca^{2+}]_{ec}$ is not as great on Q as on P_r , it does mean that attempts to measure the cooperativity of Ca^{2+} in central synaptic release need to be interpreted with caution,

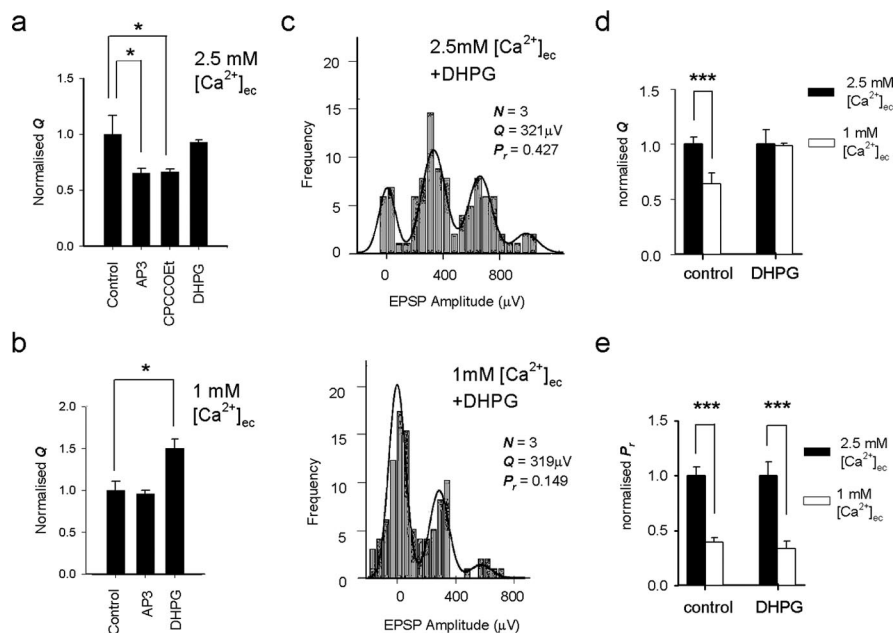


Figure 5. Regulation of Q by extracellular Ca^{2+} is mediated by mGluR1. *a*, Summary data of recordings made in 2.5 mM $[Ca^{2+}]_{ec}$ showing the effect of AP3 (1 mM; $n = 7$), CPCCOEt (50 μ M; $n = 3$), and DHPG (100 μ M; $n = 10$) on quantal size. *b*, Summary data of recordings made in 1 mM $[Ca^{2+}]_{ec}$ showing the effect of AP3 (1 mM; $n = 5$) and DHPG (100 μ M; $n = 5$) on quantal size. *c*, EPSP amplitude frequency histograms from recordings made first in 2.5 mM (top) and then 1 mM Ca^{2+} (bottom), in the continued presence of DHPG, taken from a single experiment. The model fit for each distribution is indicated by a solid line, with derived values of N , P_r , and Q shown. *d*, Summary data from six recordings showing that DHPG prevents the drop in Q when $[Ca^{2+}]_{ec}$ is reduced from 2.5 to 1 mM. *e*, Summary data from six recordings showing that DHPG does not prevent the drop in P_r when $[Ca^{2+}]_{ec}$ is lowered from 2.5 to 1 mM. Error bars indicate SE. *** $p < 0.001$.

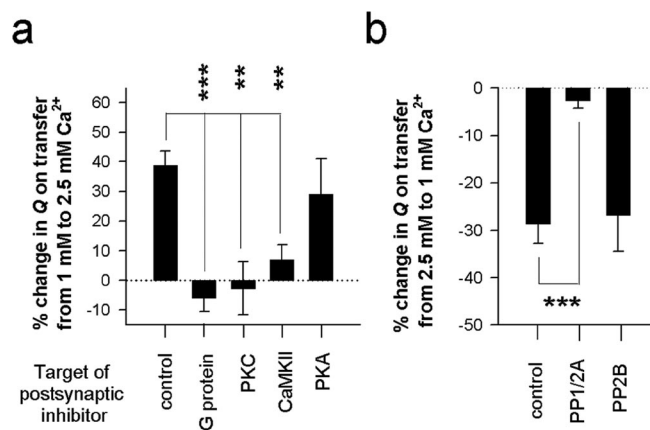


Figure 6. The effect on Q is mediated by canonical type 1 mGluR signaling. *a*, Summary data showing the effect of the G-protein inhibitor (pertussis toxin, 1 μ g/ml; $n = 5$), the PKC inhibitor (GF109203X, 100 μ M; $n = 5$), the CaMKII inhibitor (KN62, 50 μ M; $n = 4$), and the PKA inhibitor (H9, 10 μ M; $n = 4$) on preventing the increase in quantal size (Q) observed under control conditions when $[Ca^{2+}]_{ec}$ is raised from 1 to 2.5 mM. Results are expressed as the percentage increase in Q measured in 2.5 mM Ca^{2+}_{ec} compared with that recorded in 1 mM Ca^{2+}_{ec} . *b*, Summary data showing the effect of the protein phosphatase blockers microcystin (10 μ M; $n = 4$) and cyclosporin (10 μ M; $n = 4$) on preventing the reduction in quantal size (Q) observed under control conditions when $[Ca^{2+}]_{ec}$ is reduced from 2.5 to 1 mM. Results are expressed as the percentage reduction in Q measured in 1 mM Ca^{2+}_{ec} compared with that measured in 2.5 mM Ca^{2+}_{ec} . Error bars indicate SE. *** $p < 0.001$; ** $p < 0.01$.

particularly where release is measured postsynaptically (Goda and Stevens, 1994; Mintz et al., 1995; Qian and Noebels, 2001). Nevertheless, the wide range in cooperativity values obtained at central synapses, from 1 (Augustine, 1990) to 3.5 and 4 (Goda and Stevens, 1994; Qian and Noebels, 2001) are unlikely to be

explained by the postsynaptic effect on Q that we have reported. A more likely explanation of these observations is that synaptic release machinery can operate with different levels of cooperativity at the same synapse (the Calyx of Held), depending on the intracellular $[Ca^{2+}]_i$ ($[Ca^{2+}]_{ic}$) after stimulation (Lou et al., 2005).

In our data, the dependence of synaptic release (P_r) on $[Ca^{2+}]_{ec}$ is close to linear ($n = 1.03$), whereas the effect on Q ($n = 0.44$) is sublinear. The overall cooperativity at these synapses is close to 1.5, as a result of both of these effects.

The mechanism for the change in quantal size

The identification of cell surface detectors of Ca^{2+}_{ec} has put forward the question of whether Ca^{2+} also functions as an extracellular signaling molecule in the brain (Bouschet and Henley, 2005). The prototypical Ca^{2+}_{ec} sensing receptor (CaR) was initially cloned in the parathyroid gland (Brown et al., 1993) and is expressed in varying amounts in many tissues, including the CNS, specifically concentrated at nerve terminals (Ruat et al., 1995). Group 1 mGluRs are structurally similar to CaR (Hermans and Challiss, 2001), both operate via G-proteins (Brown and MacLeod, 2001), and have been reported to also have significant sensitivity to $[Ca^{2+}]_{ec}$ (Kubo et al., 1998; Francesconi and Duvoisin, 2004). Heterodimerization of CaR with Group 1 mGluRs has also been shown to take place in hippocampal and cerebellar neurons (Gama et al., 2001). An important question to ask will be whether CaR heterodimerizes to mGluRs in the intact brain or whether mGluR expresses its sensitivity to Ca^{2+} without binding to CaR.

Other divalent cations (e.g., Mg^{2+} , Zn^{2+}) have also been shown to activate mGluRs in combination with glutamate (Francesconi and Duvoisin, 2004), which is consistent with the results from this study where Mg^{2+} can prevent the drop in Q at low $[Ca^{2+}]_{ec}$ (Fig. 4) and may explain why the Q reduction has not been observed previously, as Ca^{2+} is often replaced with Mg^{2+} at reduced $[Ca^{2+}]_{ec}$ (Silver et al., 1996). More recent work suggests that changes in $[Ca^{2+}]_{ec}$ can alter the range of concentrations of agonist to which the group 1 metabotropic glutamate receptor (mGluR1) responds (Tabata et al., 2002), shifting the dynamic range to include lower concentrations by up to 100-fold. Because DHPG and glutamate have similar agonist affinities (Conn and Pin, 1997), this implies that at resting concentrations of Ca^{2+} (1.5–2 mM) (Cohen and Fields, 2004) and glutamate (0.5–2 μ M) (Meldrum, 2000; Cavalier et al., 2005), a significant percentage of the mGluR1 receptors may be “constitutively” active, but become inactivated as $[Ca^{2+}]_{ec}$ is lowered.

In the CNS, a variety of effects produced by mGluR1 have been described. The group 1 mGluRs (mGluR1 and mGluR5) activate CaMKII and PKC via phospholipase $C\alpha$ (Berridge and Irvine, 1984; Hermans and Challiss, 2001). Activated CaMKII and PKC have both been shown to phosphorylate AMPA receptors on the serine 831 (s831) site (Tan et al., 1994; Barria et al., 1997; Mammen et al., 1997), which increases the single channel current. The average increase in mean AMPA channel conductance from either CaMKII or PKC is of the order of 30–40% (Carroll et al., 1998; Derkach et al., 1999), and basal phosphorylation of the s831 site has been suggested (Mammen et al., 1997). The drop in Q we observed on reducing $[Ca^{2+}]_{ec}$ to 1 mM was 36%, with a comparable drop in the mean amplitude of mEPSPs (32%). This approximate alignment in the magnitude of the change, coupled with the effects of CaMKII and PKC antagonists, strongly suggests that the drop in Q at lowered $[Ca^{2+}]_{ec}$ is ex-

plained by a loss of AMPA receptor phosphorylation at the s831 site.

Although our results suggest that the effect of $[Ca^{2+}]_{ec}$ on Q is mediated by postsynaptic mGluRs, another possibility is that Ca^{2+} is having a direct effect on the AMPA current. However, the Ca^{2+} permeability of AMPA receptors in pyramidal neurons of rat neocortex of similar age to that used in our study has been shown to be low [ratio of Ca^{2+} to monovalent permeability of ~ 0.05 (Jonas et al., 1994)], suggesting that it is unlikely that the reduction in quantal size we observed in this study at lowered $[Ca^{2+}]_{ec}$ is caused by a reduction in Ca^{2+} ions flowing through AMPA channels.

Another possibility is that Ca^{2+} is having a direct modulatory effect at the AMPA receptor. Recently it has been demonstrated that divalent cations can act like competitive antagonists at the AMPA receptor (Dorofeeva et al., 2005). The effect we report in this study is a reduction in AMPA current with lowering of $[Ca^{2+}]_{ec}$. This is the opposite of what would be expected if Ca^{2+} was acting as an antagonist, and therefore cannot explain our observations.

A further possibility is that the reduction in Q is caused by a diminished release of transmitter from the vesicle, akin to the mechanisms discussed by Chen et al. (2004). There is clear evidence at some central synapses (cerebellum, hippocampus, Calyx of Held) that activation of mGluR1 can cause a presynaptic inhibition, arising from the postsynaptic release of endocannabinoids (Morishita et al., 1998; Maejima et al., 2001; Kushmerick et al., 2004). Decreases in $[Ca^{2+}]_{ec}$ have been shown to activate voltage-dependent outward currents in synaptosomes and may, in this way, modulate the excitability of the presynaptic terminal (Smith et al., 2004). Our results (including mEPSP analysis) are not readily compatible with a presynaptic mechanism, as it might be expected that the degree of glutamate release from an individual vesicle would also be linked to a change in P_r (for a discussion of mechanisms, see Chen et al., 2004); in our experiments, neither agonist nor antagonist produced a consistent change in P_r at either 1 or 2.5 mM $[Ca^{2+}]_{ec}$, so we regard a presynaptic explanation of the change in Q as highly unlikely.

Does the mechanism for change in Q operate physiologically?

The rationale for performing our experiments was that there was evidence that $[Ca^{2+}]_{ec}$ can fall during normal physiological function (Massimini and Amzica, 2001; Cohen and Fields, 2004). We therefore explored the effect of lowered $[Ca^{2+}]_{ec}$ without reproducing the exact physiological circumstances in which this effect is reported to occur. The lowered $[Ca^{2+}]_{ec}$ effect normally occurs after a period of excitatory synaptic activity, particularly if there is sufficient excitatory depolarization to cause inward current through the NMDA receptors (Rusakov and Fine, 2003). We have interpreted our data as implying that a fall in $[Ca^{2+}]_{ec}$ may lower the sensitivity of the mGluR1 to ambient agonists (i.e., glutamate) and, hence, reduce activation of the mGluR1 receptor.

However, the decrease in $[Ca^{2+}]_{ec}$ is evoked by release of glutamate and, hence, occurs in circumstances when $[glut]_{ec}$ should be raised. Thus, initially these two extracellular effects may cancel each other out and the possibility of decreased activation of the mGluR1 would only occur if the decreased $[Ca^{2+}]_{ec}$ outlasted the increased $[glut]_{ec}$. Both modeling and experimental studies indicate that is indeed likely to occur, providing the $[Ca^{2+}]_{ec}$ depletion is partly caused by functional activation of the NMDA receptors, because elevated $[glut]_{ec}$ is relatively rapidly cleared by the glutamate transporter, whereas the Ca^{2+} depletion

can continue for longer than 100 ms. (Rusakov, 2001; Rusakov and Fine, 2003). The kinetics for activation and deactivation of mGluR1 are not known, but there may be an adequate period of lowered $[Ca^{2+}]_{ec}$ in near normal ambient glutamate to allow for deactivation of the mechanism. Further exploration of the mechanism would be desirable, not only in terms of the kinetics, but also with respect to the effect of different levels of the ambient agonists; GABA may also extend sensitivity of the receptor to glutamate (Tabata et al., 2004). This may be fundamental to the type and duration of plasticity induced in an experimental preparation (Braunewell et al., 2003; van Dam et al., 2004) because there is some evidence that *in vitro* and *in vivo* preparations may have different ambient levels of transmitters such as glutamate (Cavelier et al., 2005). This may in turn be one contributing factor in explaining the diversity of results that have been obtained for long-term potentiation and long-term depression experiments (van Dam et al., 2004).

References

- Augustine GJ (1990) Regulation of transmitter release at the squid giant synapse by presynaptic delayed rectifier potassium current. *J Physiol (Lond)* 431:343–364.
- Augustine GJ (2001) How does calcium trigger neurotransmitter release? *Curr Opin Neurobiol* 11:320–326.
- Bandrowski AE, Aramakis VB, Moore SL, Ashe JH (2001) Metabotropic glutamate receptors modify ionotropic glutamate responses in neocortical pyramidal cells and interneurons. *Exp Brain Res* 136:25–40.
- Barria A, Derkach V, Soderling T (1997) Identification of the Ca^{2+} /calmodulin-dependent protein kinase II regulatory phosphorylation site in the alpha-amino-3-hydroxy-5-methyl-4-isoxazole-propionate-type glutamate receptor. *J Biol Chem* 272:32727–32730.
- Berridge MJ, Irvine RF (1984) Inositol trisphosphate, a novel second messenger in cellular signal transduction. *Nature* 312:315–321.
- Borst JG, Sakmann B (1999) Depletion of calcium in the synaptic cleft of a calyx-type synapse in the rat brainstem. *J Physiol (Lond)* 521:123–133.
- Bouschet T, Henley JM (2005) Calcium as an extracellular signalling molecule: perspectives on the calcium sensing receptor in the brain. *C R Biol* 328:691–700.
- Braunewell KH, Brackmann M, Manahan-Vaughan D (2003) Group I mGlu receptors regulate the expression of the neuronal calcium sensor protein VILIP-1 *in vitro* and *in vivo*: implications for mGlu receptor-dependent hippocampal plasticity? *Neuropharmacology* 44:707–715.
- Brown EM, MacLeod RJ (2001) Extracellular calcium sensing and extracellular calcium signaling. *Physiol Rev* 81:239–297.
- Brown EM, Gamba G, Riccardi D, Lombardi M, Butters R, Kifor O, Sun A, Hediger MA, Lytton J, Hebert SC (1993) Cloning and characterization of an extracellular Ca^{2+} -sensing receptor from bovine parathyroid. *Nature* 366:575–580.
- Carroll RC, Nicoll RA, Malenka RC (1998) Effects of PKA and PKC on miniature excitatory postsynaptic currents in CA1 pyramidal cells. *J Neurophysiol* 80:2797–2800.
- Cavelier P, Hamann M, Rossi D, Mobbs P, Attwell D (2005) Tonic excitation and inhibition of neurons: ambient transmitter sources and computational consequences. *Prog Biophys Mol Biol* 87:3–16.
- Chen G, Harata NC, Tsien RW (2004) Paired-pulse depression of unitary quantal amplitude at single hippocampal synapses. *Proc Natl Acad Sci USA* 101:1063–1068.
- Cohen JE, Fields RD (2004) Extracellular calcium depletion in synaptic transmission. *Neuroscientist* 10:12–17.
- Conn PJ, Pin JP (1997) Pharmacology and functions of metabotropic glutamate receptors. *Annu Rev Pharmacol Toxicol* 37:205–237.
- Del Castillo J, Katz B (1954) Quantal components of the end-plate potential. *J Physiol (Lond)* 124:560–573.
- Derkach V, Barria A, Soderling TR (1999) Ca^{2+} /calmodulin-kinase II enhances channel conductance of alpha-amino-3-hydroxy-5-methyl-4-isoxazolepropionate type glutamate receptors. *Proc Natl Acad Sci USA* 96:3269–3274.
- Doty HU, Zieglansberger W (1990) Visualizing unstained neurons in living brain slices by infrared DIC-videomicroscopy. *Brain Res* 537:333–336.
- Dorofeeva NA, Tikhonov DB, Barygin OI, Tikhonova TB, Salnikov YI, Magazanik LG (2005) Action of extracellular divalent cations on native alpha-amino-3-hydroxy-5-methylisoxazole-4-propionate (AMPA) receptors. *J Neurochem* 95:1704–1712.
- Egelman DM, Montague PR (1998) Computational properties of peridendritic calcium fluctuations. *J Neurosci* 18:8580–8589.
- Egelman DM, Montague PR (1999) Calcium dynamics in the extracellular space of mammalian neural tissue. *Biophys J* 76:1856–1867.
- Feldmeyer D, Egger V, Lubke J, Sakmann B (1999) Reliable synaptic connections between pairs of excitatory layer 4 neurones within a single “barrel” of developing rat somatosensory cortex. *J Physiol (Lond)* 521:169–190.
- Francesconi A, Duvoisin RM (2004) Divalent cations modulate the activity of metabotropic glutamate receptors. *J Neurosci Res* 75:472–479.
- Gama L, Wilt SG, Breitwieser GE (2001) Heterodimerization of calcium sensing receptors with metabotropic glutamate receptors in neurons. *J Biol Chem* 276:39053–39059.
- Goda Y, Stevens CF (1994) Two components of transmitter release at a central synapse. *Proc Natl Acad Sci USA* 91:12942–12946.
- Gudermann T, Kalkbrenner F, Schultz G (1996) Diversity and selectivity of receptor-G protein interaction. *Annu Rev Pharmacol Toxicol* 36:429–459.
- Hardingham NR, Larkman AU (1998) Rapid report: the reliability of excitatory synaptic transmission in slices of rat visual cortex *in vitro* is temperature dependent. *J Physiol (Lond)* 507:249–256.
- Hermans E, Challiss RA (2001) Structural, signalling and regulatory properties of the group I metabotropic glutamate receptors: prototypic family C G-protein-coupled receptors. *Biochem J* 359:465–484.
- Hille B, Woodhull AM, Shapiro BI (1975) Negative surface charge near sodium channels of nerve: divalent ions, monovalent ions, and pH. *Philos Trans R Soc Lond B Biol Sci* 270:301–318.
- Iserhot C, Gebhardt C, Schmitz D, Heinemann U (2004) Glutamate transporters and metabotropic receptors regulate excitatory neurotransmission in the medial entorhinal cortex of the rat. *Brain Res* 1027:151–160.
- Jin XT, Beaver CJ, Ji Q, Daw NW (2001) Effect of the group I metabotropic glutamate agonist DHPG on the visual cortex. *J Neurophysiol* 86:1622–1631.
- Jonas P, Racca C, Sakmann B, Seeburg PH, Monyer H (1994) Differences in Ca^{2+} permeability of AMPA-type glutamate receptor channels in neocortical neurons caused by differential GluR-B subunit expression. *Neuron* 12:1281–1289.
- Koester HJ, Johnston D (2005) Target cell-dependent normalization of transmitter release at neocortical synapses. *Science* 308:863–866.
- Kubo Y, Miyashita T, Murata Y (1998) Structural basis for a Ca^{2+} -sensing function of the metabotropic glutamate receptors. *Science* 279:1722–1725.
- Kushmerick C, Price GD, Taschenberger H, Puente N, Renden R, Wadiche JI, Duvoisin RM, Grandes P, von Gersdorff H (2004) Retroinhibition of presynaptic Ca^{2+} currents by endocannabinoids released via postsynaptic mGluR activation at a calyx synapse. *J Neurosci* 24:5955–5965.
- Larkman AU, Jack JJ, Stratford KJ (1997) Quantal analysis of excitatory synapses in rat hippocampal CA1 *in vitro* during low-frequency depression. *J Physiol (Lond)* 505:457–471.
- Lou X, Scheuss V, Schneggenburger R (2005) Allosteric modulation of the presynaptic Ca^{2+} sensor for vesicle fusion. *Nature* 435:497–501.
- Lujan R, Roberts JD, Shigemoto R, Ohishi H, Somogyi P (1997) Differential plasma membrane distribution of metabotropic glutamate receptors mGluR1 alpha, mGluR2 and mGluR5, relative to neurotransmitter release sites. *J Chem Neuroanat* 13:219–241.
- Maejima T, Hashimoto K, Yoshida T, Aiba A, Kano M (2001) Presynaptic inhibition caused by retrograde signal from metabotropic glutamate to cannabinoid receptors. *Neuron* 31:463–475.
- Mammen AL, Kameyama K, Roche KW, Hagan RL (1997) Phosphorylation of the alpha-amino-3-hydroxy-5-methylisoxazole-4-propionic acid receptor GluR1 subunit by calcium/calmodulin-dependent kinase II. *J Biol Chem* 272:32528–32533.
- Markram H, Lubke J, Frotscher M, Roth A, Sakmann B (1997) Physiology and anatomy of synaptic connections between thick tufted pyramidal neurones in the developing rat neocortex. *J Physiol (Lond)* 500:409–440.
- Mason A, Nicoll A, Stratford K (1991) Synaptic transmission between individual pyramidal neurons of the rat visual cortex *in vitro*. *J Neurosci* 11:72–84.

- Massimini M, Amzica F (2001) Extracellular calcium fluctuations and intracellular potentials in the cortex during the slow sleep oscillation. *J Neurophysiol* 85:1346–1350.
- McCormick DA, Connors BW, Lighthall JW, Prince DA (1985) Comparative electrophysiology of pyramidal and sparsely spiny stellate neurons of the neocortex. *J Neurophysiol* 54:782–806.
- Meldrum BS (2000) Glutamate as a neurotransmitter in the brain: review of physiology and pathology. *J Nutr* 130:1007S–1015S.
- Mintz IM, Sabatini BL, Regehr WG (1995) Calcium control of transmitter release at a cerebellar synapse. *Neuron* 15:675–688.
- Morishita W, Kirov SA, Alger BE (1998) Evidence for metabotropic glutamate receptor activation in the induction of depolarization-induced suppression of inhibition in hippocampal CA1. *J Neurosci* 18:4870–4882.
- Nicholson C, Bruggencate GT, Steinberg R, Stockle H (1977) Calcium modulation in brain extracellular microenvironment demonstrated with ion-selective micropipette. *Proc Natl Acad Sci USA* 74:1287–1290.
- Press WH, Teukolsky SA, Vetterling WT, Flannery BP (1993) Numerical recipes in C, Ed 2. Cambridge, UK: Cambridge UP.
- Pumain R, Heinemann U (1985) Stimulus- and amino acid-induced calcium and potassium changes in rat neocortex. *J Neurophysiol* 53:1–16.
- Qian J, Noebels JL (2001) Presynaptic Ca^{2+} channels and neurotransmitter release at the terminal of a mouse cortical neuron. *J Neurosci* 21:3721–3728.
- Ruat M, Molliver ME, Snowman AM, Snyder SH (1995) Calcium sensing receptor: molecular cloning in rat and localization to nerve terminals. *Proc Natl Acad Sci USA* 92:3161–3165.
- Rusakov DA (2001) The role of perisynaptic glial sheaths in glutamate spillover and extracellular Ca^{2+} depletion. *Biophys J* 81:1947–1959.
- Rusakov DA, Fine A (2003) Extracellular Ca^{2+} depletion contributes to fast activity-dependent modulation of synaptic transmission in the brain. *Neuron* 37:287–297.
- Rusakov DA, Kullmann DM, Stewart MG (1999) Hippocampal synapses: do they talk to their neighbours? *Trends Neurosci* 22:382–388.
- Silver RA, Cull-Candy SG, Takahashi T (1996) Non-NMDA glutamate receptor occupancy and open probability at a rat cerebellar synapse with single and multiple release sites. *J Physiol (Lond)* 494:231–250.
- Silver RA, Lubke J, Sakmann B, Feldmeyer D (2003) High-probability unquantal transmission at excitatory synapses in barrel cortex. *Science* 302:1981–1984.
- Smith SM, Bergsman JB, Harata NC, Scheller RH, Tsien RW (2004) Recordings from single neocortical nerve terminals reveal a nonselective cation channel activated by decreases in extracellular calcium. *Neuron* 41:243–256.
- Stricker C, Redman SJ (2003) Quantal analysis based on density estimation. *J Neurosci Methods* 130:159–171.
- Stricker C, Field AC, Redman SJ (1996) Statistical analysis of amplitude fluctuations in EPSCs evoked in rat CA1 pyramidal neurones in vitro. *J Physiol (Lond)* 490:419–441.
- Tabata T, Aiba A, Kano M (2002) Extracellular calcium controls the dynamic range of neuronal metabotropic glutamate receptor responses. *Mol Cell Neurosci* 20:56–68.
- Tabata T, Araishi K, Hashimoto K, Hashimoto Y, van der Putten H, Bettler B, Kano M (2004) Ca^{2+} activity at $GABA_B$ receptors constitutively promotes metabotropic glutamate signaling in the absence of GABA. *Proc Natl Acad Sci USA* 101:16952–16957.
- Tan SE, Wenthold RJ, Soderling TR (1994) Phosphorylation of AMPA-type glutamate receptors by calcium/calmodulin-dependent protein kinase II and protein kinase C in cultured hippocampal neurons. *J Neurosci* 14:1123–1129.
- Thomas GD, O'Rourke B, Sikkink R, Rusnak F, Marban E, Victor RG (1997) Differential modulation of cortical synaptic activity by calcineurin (phosphatase 2B) versus phosphatases 1 and 2A. *Brain Res* 749:101–108.
- van Dam EJ, Kamal A, Artola A, de Graan PN, Gispen WH, Ramakers GM (2004) Group I metabotropic glutamate receptors regulate the frequency-response function of hippocampal CA1 synapses for the induction of LTP and LTD. *Eur J Neurosci* 19:112–118.
- Vassilev PM, Mitchel J, Vassilev M, Kanazirska M, Brown EM (1997) Assessment of frequency-dependent alterations in the level of extracellular Ca^{2+} in the synaptic cleft. *Biophys J* 72:2103–2116.
- Wall MJ, Usowicz MM (1998) Development of the quantal properties of evoked and spontaneous synaptic currents at a brain synapse. *Nat Neurosci* 1:675–682.
- Walmsley B, Edwards FR, Tracey DJ (1988) Nonuniform release probabilities underlie quantal synaptic transmission at a mammalian excitatory central synapse. *J Neurophysiol* 60:889–908.
- Wang XF, Daw NW (1996) Metabotropic glutamate receptors potentiate responses to NMDA and AMPA from layer V cells in rat visual cortex. *J Neurophysiol* 76:808–815.
- Wiest MC, Eagleman DM, King RD, Montague PR (2000) Dendritic spikes and their influence on extracellular calcium signaling. *J Neurophysiol* 83:1329–1337.